Supplementary Figure 1 Dronamraju *et al.*

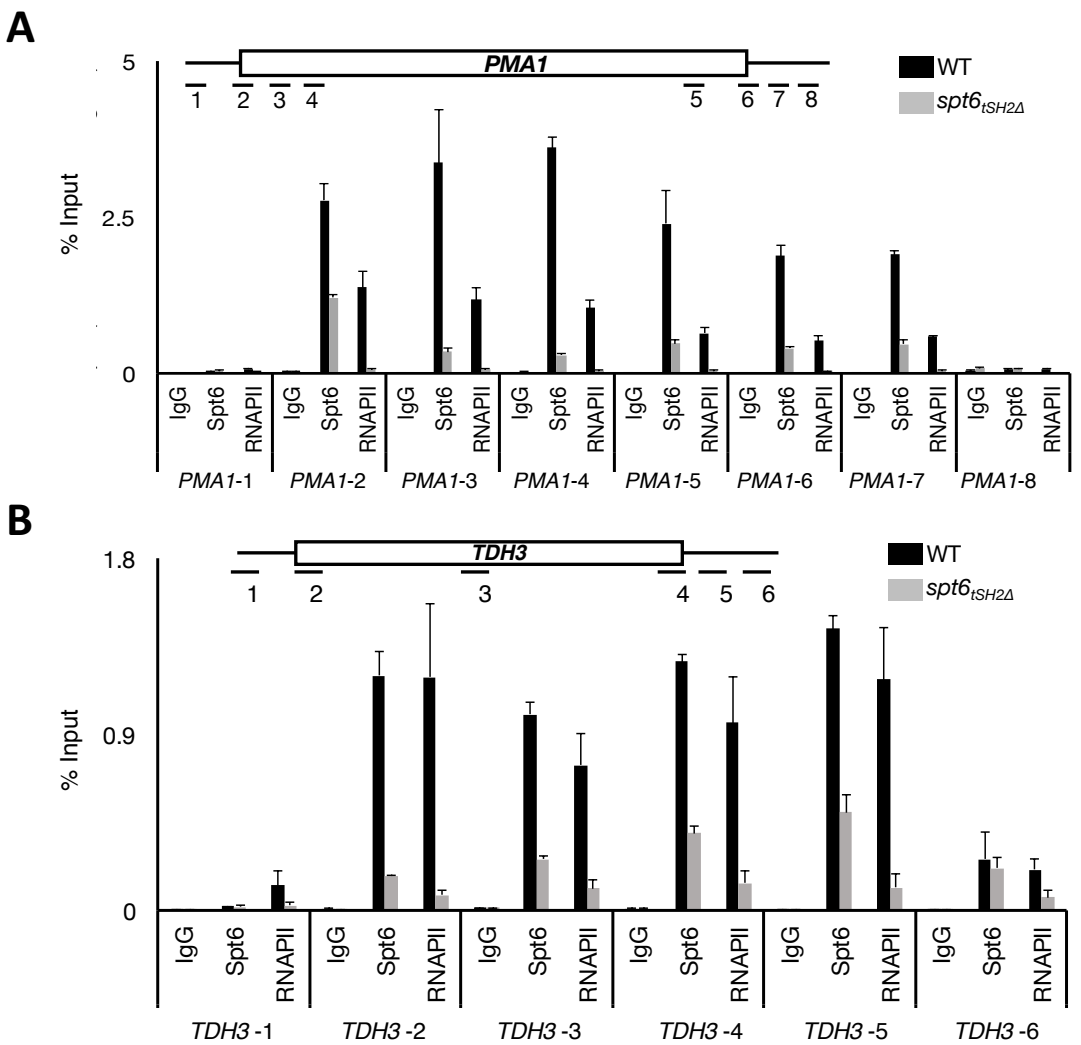

Supplementary Figure 2 Dronamraju *et al.*

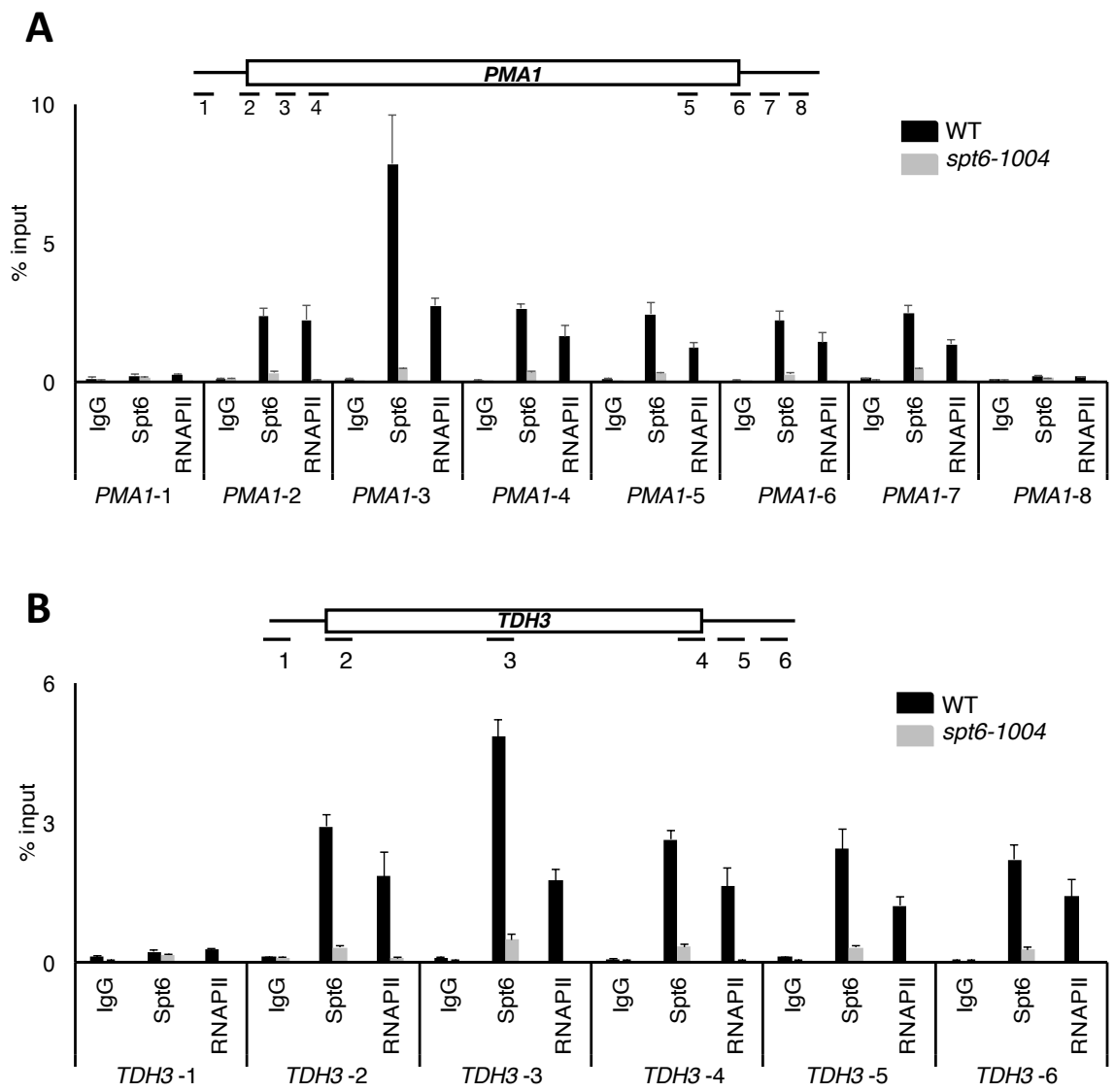

Supplementary Figure 3 Dronamraju *et al.*

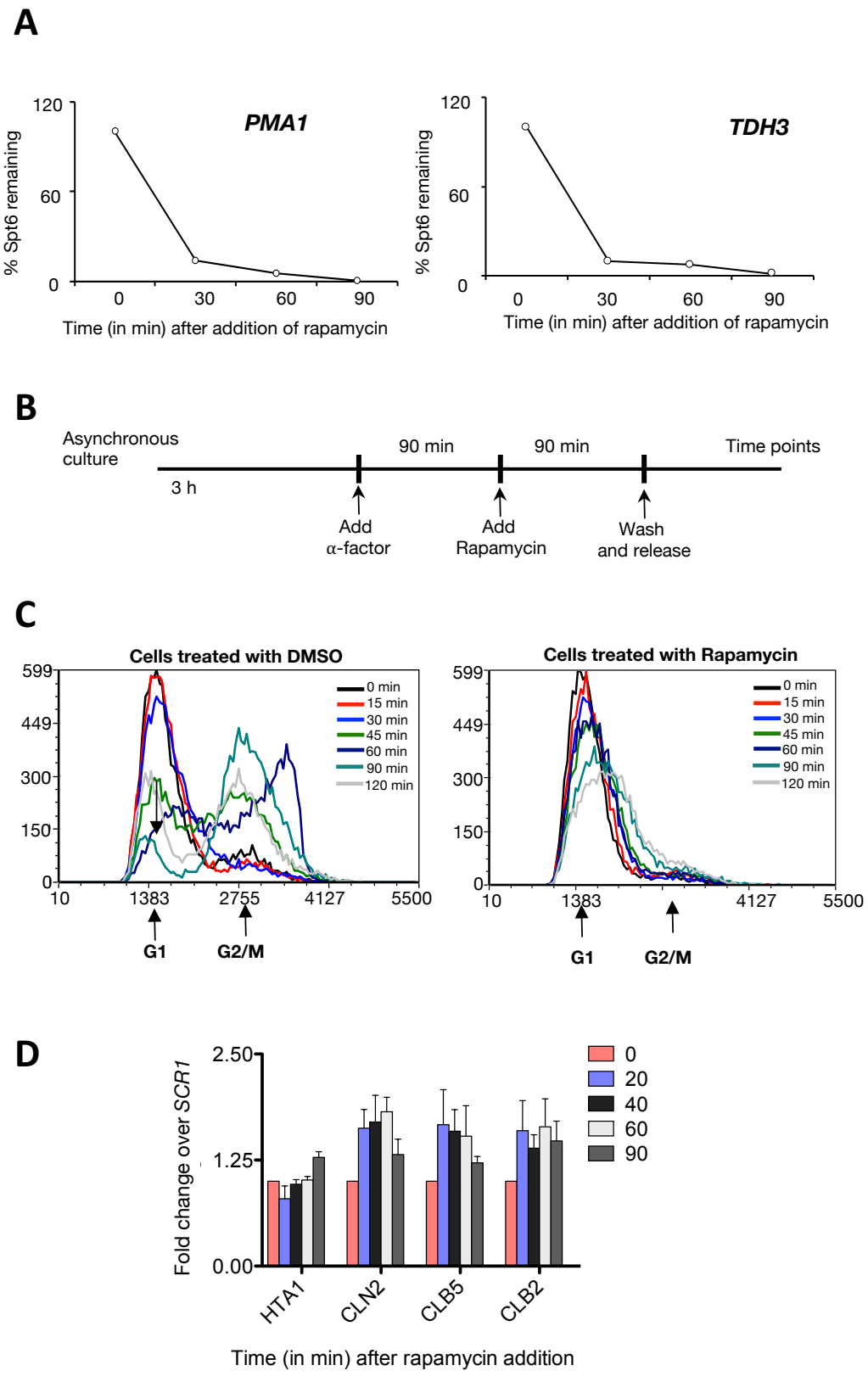

Supplementary Figure 4 Dronamraju *et al.*

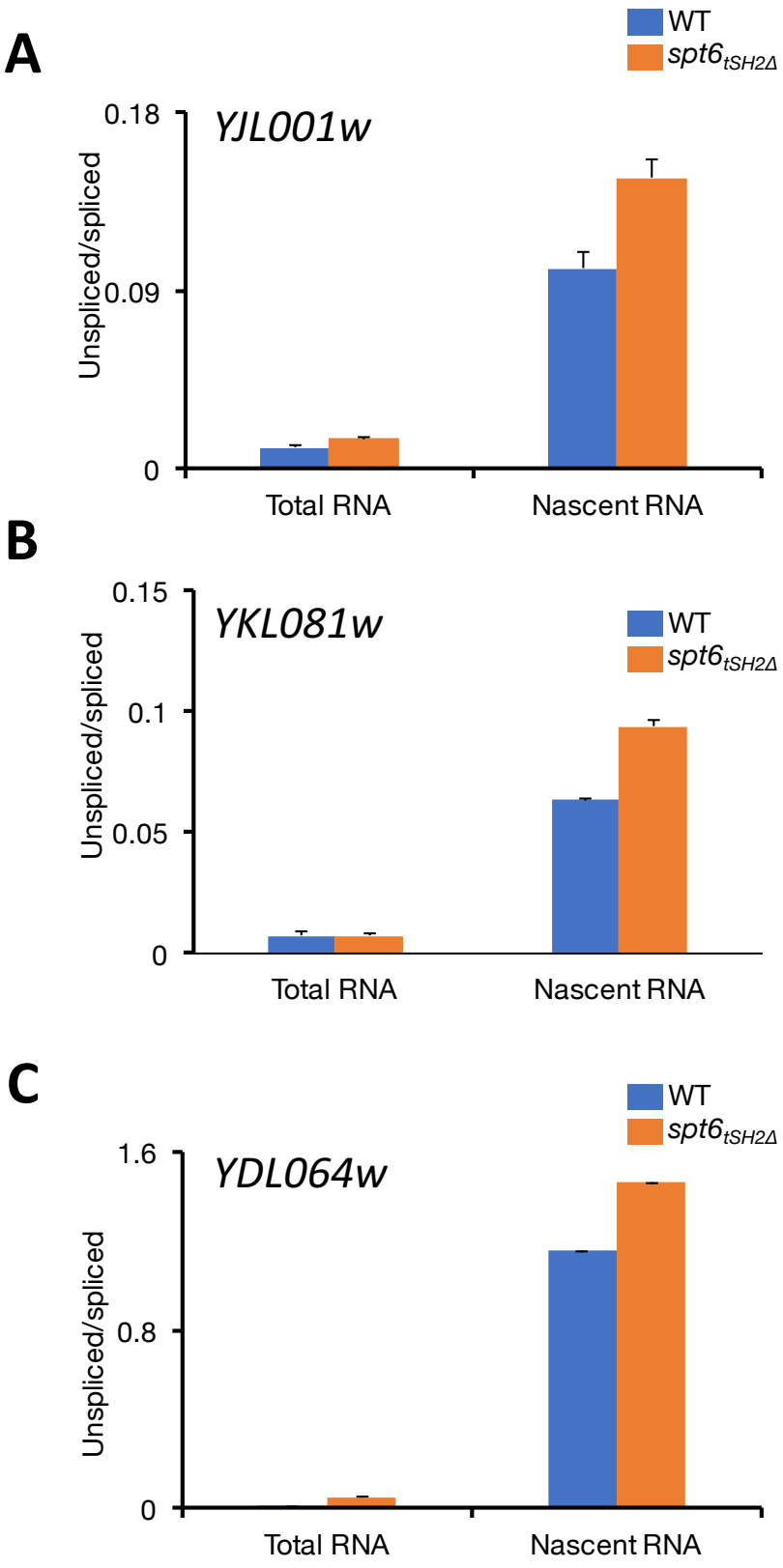

Supplementary Figure 5 Dronamraju *et al.*

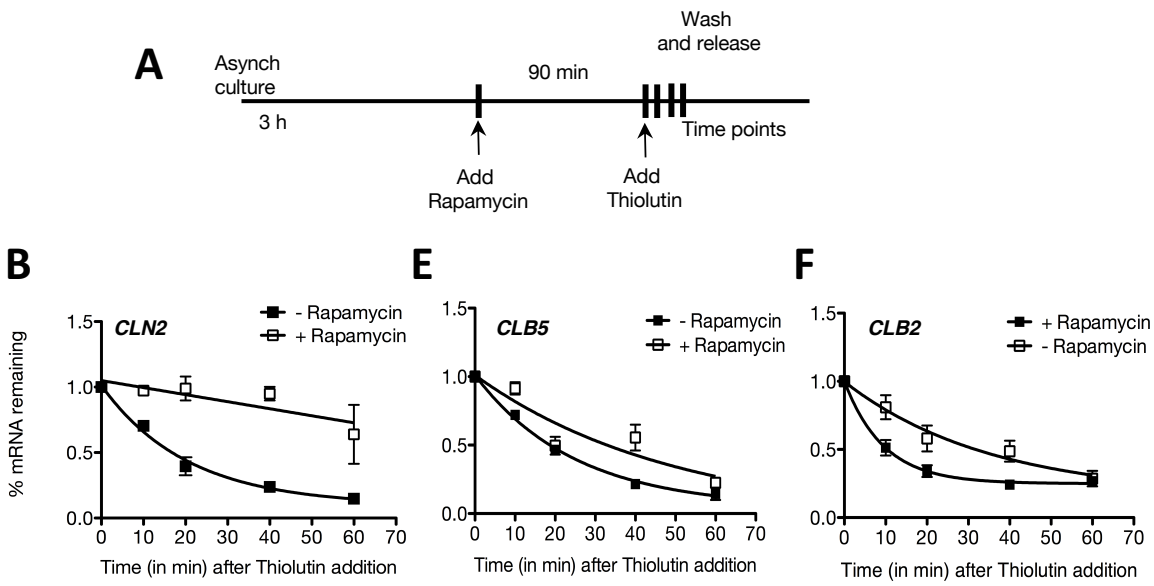

Supplementary Figure 6 Dronamraju *et al.*

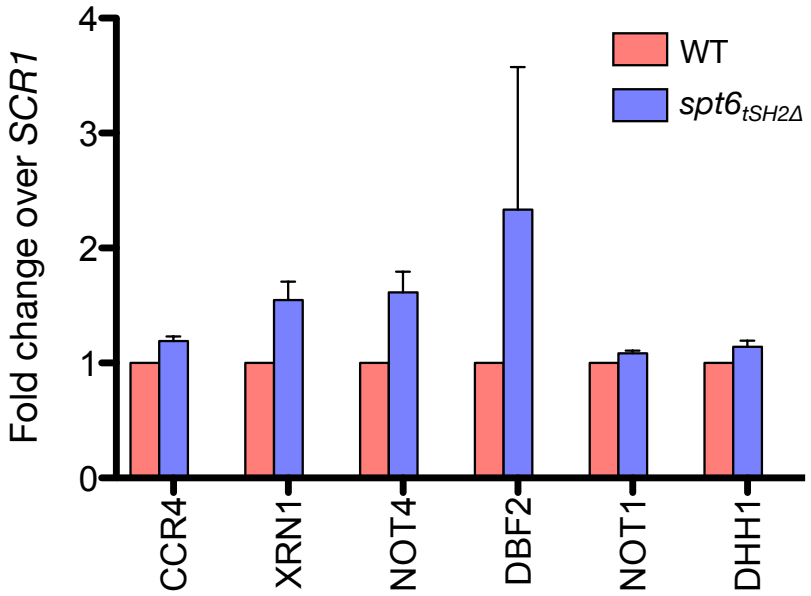

Supplementary Figure 7 Dronamraju *et al.*

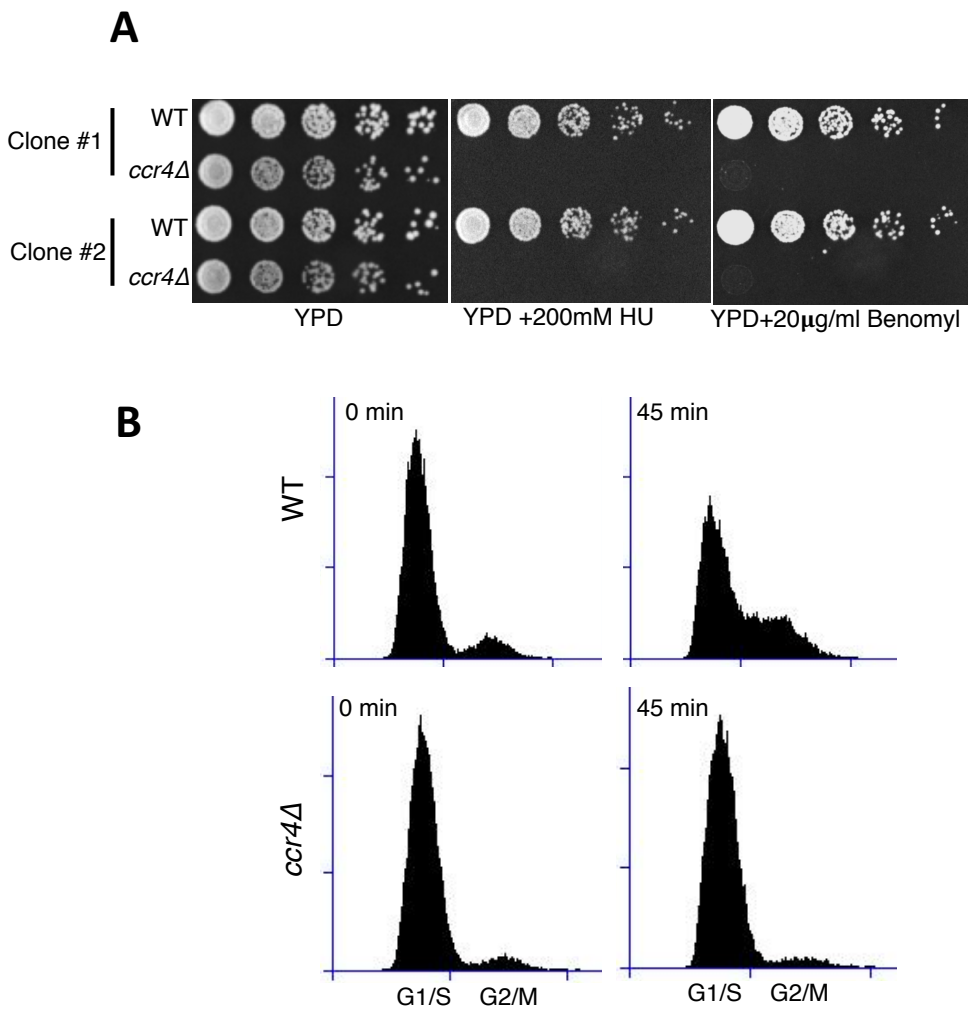

**Supplementary Figure 1. The tSH2 domain of Spt6 is required for the optimal localization of Spt6 and RNAPII on genes (Related to Figure 1)**

(A) ChIP-qPCR analysis of the distribution of Spt6 and total RNAPII at the *PMA1* locus in WT and *spt6*$_{tSH2\Delta}$ cells. Purified IgG was used as a control for the IP. Primer locations are indicated in the gene schematic. (B) Same as in (A) but for the *TDH3* gene.

**Supplementary Figure 2. Spt6 is required for the optimal localization of Spt6 and RNAPII on genes (Related to Figure 1)**

(A) ChIP-qPCR analysis of the distribution of Spt6 and total RNAPII at the *PMA1* locus in WT and *spt6-1004* cells. Purified IgG was used as a control for the IP. Primer locations are indicated in the gene schematic. (B) Same as in (A) but for the *TDH3* gene.

**Supplementary Figure 3. Nuclear depletion of Spt6 affects cell cycle progression (Related to Figure 3).**

(A) ChIP-qPCR of the percent Spt6 remaining on the *PMA1* and *TDH3* genes after rapamycin treatment at the specified intervals. (B) Experimental schematics for the treatment of cells with rapamycin and $\alpha$-factor for the cell cycle analysis. (C) Flow cytometric analysis of cells isolated at different time points after treatments as depicted in the schematic in B (D) qRT-PCR showing the alteration of transcript levels upon rapamycin-induced removal of Spt6 from the nucleus. Triplicates of three biological replicates are shown and the error bars represent the mean $\pm$ SEM.

**Supplementary Figure 4. Assessment of the purity of nascent chromatin faction (Related to Figure 5).**

RNA was extracted from the total and the nascent fractions of yeast cells (see Methods). RNA was subjected to qRT-PCR using primers described in Supplementary Table 4. (A), (B), and (C)

are the transcript ratios of unspliced over spliced for *YJL001w, YKL081w,* and *YDL064w*, respectively.

**Supplementary Figure 5. Nuclear depletion of Spt6 affects mRNA stability (Related to Figure 5).**

(A) Representation of the experimental scheme to measure time-dependent mRNA abundance following rapamycin-induced nuclear depletion of Spt6 and addition of 5 μg/ml Thiolutin to inhibit transcription. (B-D) mRNA stability of *CLN2*, *CLB5* and *CLB2* following treatment with rapamycin and Thiuolutin as depicted in C.

**Supplementary Figure 6. mRNA levels of critical factors involved in mRNA turnover (Related to Figure 5).**

Total RNA was extracted and subjected to qRT-PCR using primers described in Supplementary Table 4. Shown are the changes in the transcript ratios of critical factors governing mRNA stability.

**Supplementary Figure 7. Ccr4 is required for proper cell cycle progression (Related to Figure 5). (A)** Spotting assays showing the requirement of Ccr4 for resistance to genotoxic agents. 5-fold serial dilutions were spotted on the indicated media. Plates were incubated at 30°C and photographed after 4 days. (B) WT and *ccr4Δ* cells were arrested in G1 using α-factor and released into fresh medium; samples were collected at 30 minutes for flow cytometric analysis of DNA content.